

Accepted Manuscript

A techno-economic assessment of the potential for combining supercritical water oxidation with 'in-situ' hydrothermal synthesis of nanocatalysts using a counter current mixing reactor

Ammar Al-Atta, Thomas Huddle, Yoana García Rodríguez, Fidel Mato, Juan García-Serna, María J. Cocero, Rachel Gomes, Edward Lester

PII: S1385-8947(18)30416-9
DOI: <https://doi.org/10.1016/j.cej.2018.03.058>
Reference: CEJ 18665

To appear in: *Chemical Engineering Journal*

Received Date: 11 December 2017
Revised Date: 1 March 2018
Accepted Date: 12 March 2018

Please cite this article as: A. Al-Atta, T. Huddle, Y.G. Rodríguez, F. Mato, J. García-Serna, M.J. Cocero, R. Gomes, E. Lester, A techno-economic assessment of the potential for combining supercritical water oxidation with 'in-situ' hydrothermal synthesis of nanocatalysts using a counter current mixing reactor, *Chemical Engineering Journal* (2018), doi: <https://doi.org/10.1016/j.cej.2018.03.058>

This is a PDF file of an unedited manuscript that has been accepted for publication. As a service to our customers we are providing this early version of the manuscript. The manuscript will undergo copyediting, typesetting, and review of the resulting proof before it is published in its final form. Please note that during the production process errors may be discovered which could affect the content, and all legal disclaimers that apply to the journal pertain.



A techno-economic assessment of the potential for combining supercritical water oxidation with ‘in-situ’ hydrothermal synthesis of nanocatalysts using a counter current mixing reactor

Ammar Al-Atta¹, Thomas Huddle¹, Yoana García Rodríguez², Fidel Mato², Juan García-Serna², María J. Cocero², Rachel Gomes¹ and Edward Lester¹

¹ Department of Chemical and Environmental Engineering, University of Nottingham, University Park, Nottingham, Nottinghamshire, NG7 2RD, UK

² High Pressure Processes Group Chemical Engineering Department, University of Valladolid, Spain

edward.lester@nottingham.ac.uk ; Phone (+44) 115-951-4974

Abstract

A combined process of supercritical water oxidation (SCWO) and supercritical water hydrothermal synthesis (SCWHS) in a continuous counter current reactor is reported. Acrylic acid was used as a model unsaturated carboxylic acid compound and the effects of the reaction temperature, residence time, oxidant ratio and acrylic acid concentration on chemical oxygen demand (COD) were all investigated. Two different experimental configurations for oxidant delivery were carried out in ‘pre-heated’ and ‘non-preheated’ oxidant configurations. With a stoichiometric excess of 100% oxygen, COD reduction levels of 80% (non-preheated) and 15% (preheated) were achieved with very short residence times. SCWHS was achieved through the addition of small amounts of various soluble metal salts in the cold upflow resulted in nanoparticles forming which increased the reaction rate and hydrothermal

oxidation efficiency. The addition of small amounts of chromium nitrate (>5mM) results in nearly 100% COD reduction at 380°C and residence times of 0.75 seconds. The potential economic benefits of combining the two processes together, in the different configurations, were also evaluated.

Keywords: Supercritical Water Oxidation; Supercritical Water Hydrothermal Synthesis; Mixing; Free Hydroxyl Radicals; Homogeneous and Heterogeneous Catalysis.

1. Introduction

Research activities using supercritical water (SCW) as a reaction medium have been increasing in recent years [1-3]. The critical point for water is 374°C and 22.1MPa whereupon water exhibits unique behaviour [4]. Increasing temperature reverses the solvation properties of water and, unlike water at ambient conditions, SCW can dissolve non-polar molecules whilst also having low solubility for inorganic ionic salts. An increase in the dissociation constant (K_w) and decrease in the dielectric constant (as a result of breakage in hydrogen bonding) have a great effect on hydrolysis due to high content of H^+ and OH^- ions [5]. These characteristics create an extreme environment for most molecules and makes SCW an ideal medium for many applications including oxidation [6], composite recycling [7] and nano-particulate production [8, 9].

Supercritical water oxidation (SCWO) is a destructive process used to convert toxic and hazardous waste into less harmful products. In an ideal case this would be simply water, N_2 and CO_2 [10]. The process is well-known for its ability to destroy a wide range of complicated wastewater contaminants from a broad variety of industries [11-13]. SCWO is an alternative to combustion based technologies used for the destruction of military waste [14], resilient pesticides [13] and radioactive waste [15]. Whilst SCWO has the advantage of a higher destruction efficiency with no partial oxidation products (which can be problematic with wet air oxidation and incineration technologies) [16] there are still significant disadvantages [17]. SCWO takes place at relatively high temperatures and pressures in the presence of high oxygen concentrations and with potentially corrosive contaminants [10]. Such an environment creates challenges for process design and the choice of equipment, particularly with respect to materials of construction. Halogenated contaminants can rapidly accelerate corrosion rates [18] even with relatively expensive and exotic alloys [19].

Although the supercritical water oxidation (SCWO) has been recognized as a promising technology for hazardous waste treatment, and numerous studies on SCWO were published in last two decades, the industrial application of SCWO to-date have been limited to laboratory and pilot-plant level, and few large-scale commercial applications are reported [2]. One of the major disadvantages that inhibit the industrialization of SCWO technology is the high energy cost to get high reaction temperature (>550°C). Therefore, in order to increase the efficiency of SCWO at mild temperatures, reactive free radicals can be used as an oxidant rather than molecular oxygen. In the non-preheated H₂O₂ scenario, a highly reactive hydroxyl radical is produced via thermal decomposition as represented in Equation (1) [20, 21]. Once generated, those free radicals immediately attack all organics present in the solution as shown in Equation (2) [22].



However, when H₂O₂ is preheated in pre-heated H₂O₂ scenario, the generally accepted mechanism for the SCWO process is shown by Equation (3) [23]



At moderate temperatures (e.g. <400°C), reaction (iii) is relatively slow since ground-state oxygen does not react readily with most organic molecules because of its spin restrictions [24]. In addition, recent studies have shown that this ‘oxygenation’ accelerates the corrosion of the tubing, particularly where the H₂O₂ solution temperatures are near-critical [18, 25]. Hence, non-preheated oxidation provides a more favourable approach for SCWO.

The use of catalysts could be a means to reduce these issues, either to increase the rate of reaction or to reduce the process conditions required to achieve the same efficiency as non-catalysed reactions. Under subcritical conditions, e.g. wet air oxidation (around 300°C), the COD conversion is always lower than 70% and requires a subsequent biological treatment. The use of homogeneous or heterogeneous catalyst is restricted by the maximum metal intake of the selected bacteria. Supercritical hydrothermal synthesis (SCWHS) is another emerging technology which takes advantage of the tuneable chemical and physical properties of superheated water to produce inorganic nanoparticles by rapid nucleation [26, 27]. A wide range of metal oxide nanoparticles, titania (TiO_2), cobalt oxide (Co_3O_4), chromium oxide (Cr_2O_3), manganese oxide (MnO_2) and hematite (Fe_2O_3) have been commonly reported in the literature. The process has also been used to produce metals [28], sulphides [29], phosphates [30], as well more complex materials such as layered double hydroxides [31] and metal organic frameworks [32].

Whilst diametrically opposed as processes (one is destructive and one is for synthesis), both processes have similarities e.g. whilst there are a significant number of papers that heat the SCWO flow from ambient to supercritical conditions, using staged heating, there are others that use rapid mixing of a preheated flow (possibly containing the oxidant) with a secondary colder flow containing the contaminant [33]. The latter requires a mixing design or 'reactor' geometry and these have included co-current pipe in pipe, Y piece, tangential swirl, jetting, transpiring wall etc. The use of a reactor to mix hot and cold flows for SCWO therefore creates a valuable synergy, the opportunity for two processes at the same time. i.e. destruction of the contaminants whilst simultaneously producing nanomaterials that can act as catalysts to increase the oxidation kinetics. Certainly catalysts could be added to the contaminant flow prior to the rapid heating and oxidation phase, but this would mean pumping particulate

slurries into the system which potentially create new issues with settling [34], poor dispersion [35] and pump head wear [36].

In order to test the principle of in-situ catalyst formation during SCWO, we used acrylic acid as model unsaturated carboxylic acid contaminant. It is considered to be one of the major chemicals in a range of industries (oil additives, painting, detergents) and can cause extensive damage to the aquatic system if not being treated [37, 38]. Acrylic acid can also be considered as one of the key intermediates during phenol oxidation. In these experiments COD levels were used to quantify oxidation rates rather than measuring residual acrylic acid concentration. Measuring residual contaminant levels can give a false measure of removal efficiency since partial oxidation (to produce intermediates) is not necessarily a sufficient means of achieving COD discharge targets.

In this article, the advantages of the rapid mixing in the counter current mixing reactor [39] have been exploited to produce a combined process of organic materials oxidation and metal oxides production (in nanometre scale) which can speed up the oxidation rate via enhanced catalytic activity [40]. Furthermore, the effect of pre-heated (hot) and non-preheated (cold) hydrogen peroxide as an oxidant has been investigated.

2. Experimental

2.1 Materials

Acrylic acid, [C₃H₄O₂] (98%, extra pure) and hydrogen peroxide [H₂O₂] (30% w/v) were obtained from Fisher and were used as received without any purification. Iron(III) nitrate nonahydrate (product code: 10154170) and cobalt(II) nitrate hexahydrate (product code: 10391061) were purchased from Acros Organics. Titanium(IV) oxysulfate (product code:

495379) and chromium(III) nitrate nonahydrate (product code: 379972) were obtained from Sigma-Aldrich. Manganese(II) nitrate hexahydrate (product code: L14040) was purchased from Alfa Aesar. Distilled and deionized water ($<50\mu\text{S}/\text{cm}$) was used to make feed solutions of different molar concentrations.

2.2 Apparatus and procedures

All reactions were conducted at laboratory-scale. A simplified scheme of the experimental rig including the counter current mixing reactor is shown in Figure 1. A Gilson HPLC pumps (Model 305 equipped with a 25 SC pump head) were used for feed delivery. K type thermocouples were used for temperature monitoring at different locations. All parts, fittings and tubing were made from SS316L from Swagelok.

Two different set of experiments were carried out for investigating pre-heated and non-preheated oxidant. The methodology of reporting reaction temperature is discussed in supplementary data section S1.3.

2.2.1 Experiments with oxidant preheating

A schematic diagram for this set of experiments is shown in Figure 1a. An aqueous solution of hydrogen peroxide was preheated through 6 m length of $\frac{1}{4}$ " outer diameter (o.d.) coiled heater at supercritical temperature. This setup enabled a complete decomposition of hydrogen peroxide to supercritical water and oxygen. After the heater (insulated), the oxygen and supercritical water mixture flows downwards via the concentric tube in tube configuration (heated on the outside using a 1kW Watlow band heater) through the thinner inner tube ($\frac{1}{8}$ " o.d.), and the cold organic solution feed enters from the bottom via an outer tube ($\frac{3}{8}$ " o.d.). Mixing and oxidation reaction occurs just below down the nozzle tip [41, 42] and the product flows out of the side arm of the cross piece to the counter current heat exchanger. After cooling the product stream is brought to ambient temperature and passed through the back

pressure regulator and the liquid product flowed out at ambient conditions into collection vessel.

2.2.2 Experiments without oxidant pre-heating

In this set of experiments, free hydrogen radicals were used as an oxidant rather than oxygen gas. This was delivered as a cold feed stream containing a H_2O_2 via a third pump. This feed stream was pressurized and mixed with organic feed stream at a mixing tee below the reactor at the base, at room temperature and without any preheating. The heated SCW flow was introduced from the top as a downward flow with just deionized water (Figure 1b).

2.2.3 Experiments with in-situ catalyst addition

These experiments used the same set up as described in Section 2.2.1 and 2.2.2 but with controlled addition of different precursor salts (5, 10 and 20 mM) dissolved in 250 mL of the acrylic acid solution.

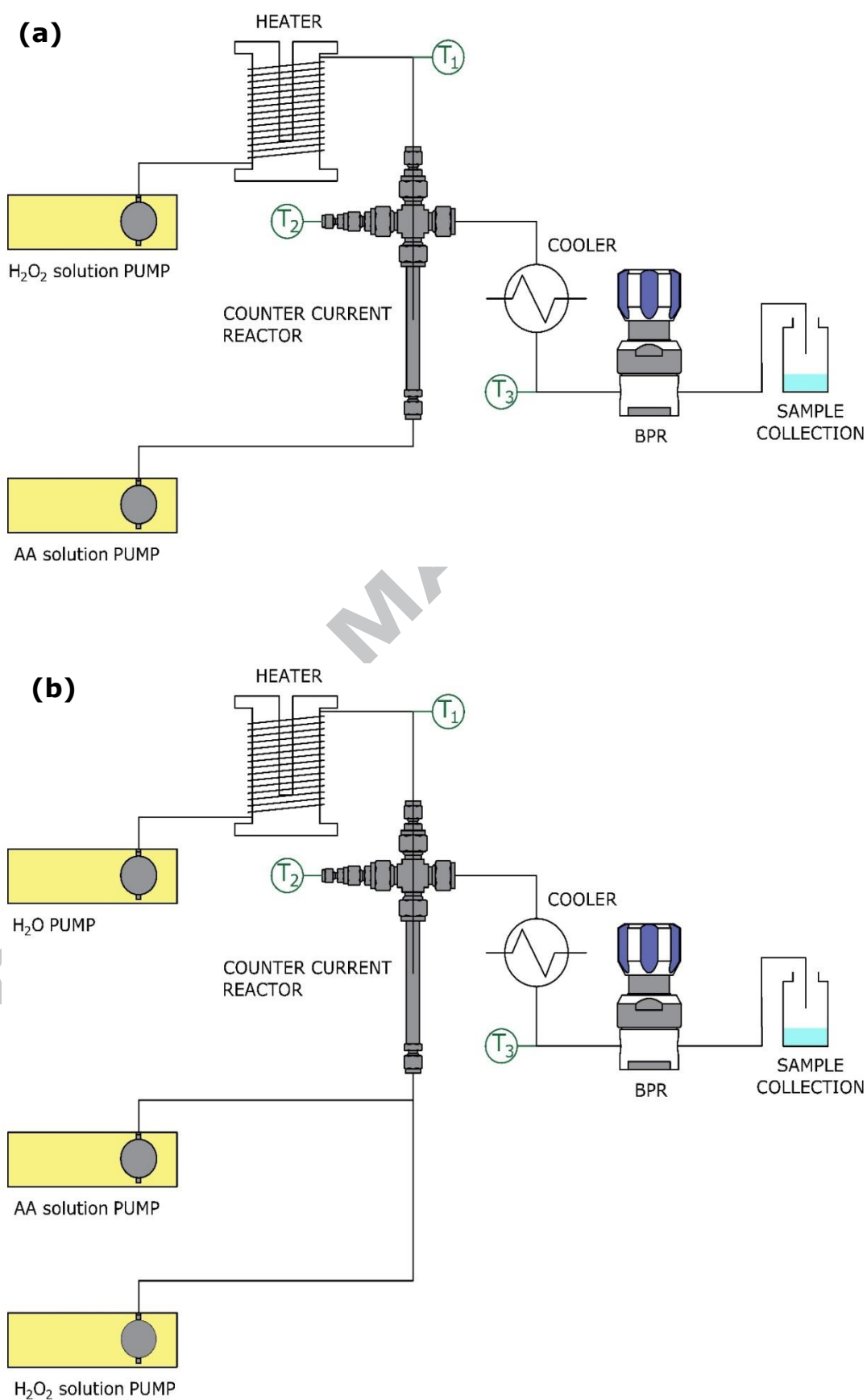


Figure 1: Flow diagram of the continuous SCWO system. (a) Preheated oxidant configuration and (b) Non-preheated oxidant configuration. T_1 measures immediately after the heater. T_2 is the post mixed flow (see Table S2 for temperatures measurements). $T_3 < 40^\circ\text{C}$, is the temperature prior to the back pressure regulator.

2.3 Analytical methods

At the end of each experiment, samples were collected and allowed to settle. The supernatants were tested for Chemical Oxygen Demand (COD) using COD cuvette test LCI400 (HACH LANGE LTD, Manchester, UK). The test involved oxidising the organic content of liquid samples under acidic conditions for 2h at 148°C. This gives water, carbon dioxide and trivalent chromium. The detection of the trivalent chromium was measured at 605 nm wavelength (DR 2800 spectrophotometer). Some researchers reported the interference of overall COD result from residual H₂O₂ in the effluent of the Advanced Oxidation Processes (AOPs)[43, 44]. Residual H₂O₂ has been found to be a problem since it will cause an overestimation of the COD. Therefore, blank tests have been carried out to ensure that all H₂O₂ has been consumed within the reactor with no residual remaining. 200% excess of H₂O₂ solutions had been mixed with supercritical water at different temperatures in non-heated oxidant configuration and the COD tests show that there is no residual H₂O₂ remaining after hydrogen peroxide decomposition test.

Samples of the nanocatalysts formed during the in-situ experiments (2.2.3) were suspended in alcohol for examination by transmission electron microscopy (TEM). A drop of this suspended alcoholic solution mixture was placed on the TEM grid. TEM images were obtained using a JEOL 2100F (FEGTEM) operating with an acceleration voltage of 100kV.

XRD analysis was carried out on the dried metal oxides nanoparticles which were obtained by freeze drying with liquid nitrogen and under low temperature vacuum (-54°C). The analysis were completed using Bruker D8 Advance (Bruker AXS, Germany) using Cu K α radiation ($\lambda=1.54056 \text{ \AA}$) in a 2θ range between 15° and 75°. Scherrer method, assuming Gaussian peak broadening was used to calculate the crystallite size for hematite, titania and cobalt oxide.

2.4 Calculations

2.4.1 Residence time

The residence time for the counter current mixing reactor was calculated to be from the mixing point, below the nozzle [39, 45] to the first cooler. The position of the mixing point is based on the pseudo reactor modelling that showed that the jetting distance relates to the flow and flow ratios [42]. The estimated average hydraulic residence time (τ) for the reaction was calculated in the following equation [46]:

$$\tau = \frac{V_r}{M_T} \rho(P, T) \quad (4)$$

Where V_r is the reaction volume, which was estimated from the mixing point of two streams to the outlet of the reactor at the top (prior to the first cooler), M_T is the total mass flow rate including the water, oxidant and the organic solution feeds into the system. The $\rho(P, T)$ term refers to the density of fluid at reaction pressure and temperature. Reaction temperature was approximated (see Figures 1a-b) from the average between the superheated water (T_1) and outlet mixture temperature (T_2).

2.4.2 Concentration of reagents at reaction conditions

The following equation is used to calculate the initial concentration of acrylic acid at the reaction conditions [47]:

$$[AA] = C_{AA} \times \frac{M_{AA}}{M_T} \times \rho(P, T) \quad (5)$$

Where, C_{AA} is the concentration of acrylic acid in the feedstock in mol/L, M_{AA} is the feed mass flow rate of acrylic acid into the reactor in g/min, M_T is the total feed mass flow rate into the system in g/min, and $\rho(P, T)$ is the density of fluid at reactions conditions.

For the initial concentration of oxidant at reaction conditions

$$[O_2] = \frac{[H_2O_2]}{2} \times \frac{M_{H_2O_2}}{M_T} \times \rho(P, T) \quad (6)$$

Where, $[H_2O_2]$ is the concentration of H_2O_2 in the feedstock in mol/L, $M_{H_2O_2}$ is the feed mass flow rate of H_2O_2 into the reactor in g/min, M_T is the total feed mass flow rate into the system in g/min, and $\rho_{(P,T)}$ is the density of fluid at reaction conditions. The equation is divided by two to fulfil the reaction stoichiometry, because 1 mole of H_2O_2 is decomposed into 0.5 mole of O_2 and 1 mole of H_2O .

2.4.3 Oxidant ratio and COD reduction

The amount of oxidant supplied for SCWO reaction is defined as follows [48]:

$$\text{Oxidant ratio} = \frac{[H_2O_2]_{initial}}{[H_2O_2]_{stoichiometric}} \quad (7)$$

The total oxidation reaction of acrylic acid to H_2O and CO_2 is presented below:



Hence, an oxidant ratio of unity indicates that the amount of oxidant delivered was exactly the amount necessary for ideal stoichiometric conversion. Consequently, an oxidant ratio greater than 1 indicates an oxygen excess and oxidant ratio less than 1 indicated an oxidant deficit.

The reduction in COD is calculated based on the following equation:

$$\%COD \text{ reduction} = \frac{COD_{inlet} - COD_{test \text{ result}}}{COD_{inlet}} \times 100 \quad (9)$$

Where COD_{inlet} and $COD_{test \text{ result}}$ are the initial and final concentrations of COD in mg/L.

Two separated streams of distilled water and a known concentration of acrylic acid in a ratio of 2:1, were flowed through the experimental rig at the beginning of operation without any pressurising or preheating. The resultant mixed solution stream was further diluted to a factor of 0.2. This 'double diluted' product represents the initial concentration of COD. The collection effluent from all SCWO experiments were diluted in the same manner.

3. Results and discussion

3.1 The effect of temperature on COD levels

Figure 2 shows the effect of reaction temperature (in the range of 300-380°C) on COD reduction at constant pressure (25.0 MPa) and stoichiometric concentration of oxidant. The flow rate and initial concentrations of reactants at the feed stock were adjusted to maintain a fixed residence time of 1.5 sec. *The impact of increasing residence time and acrylic acid concentrations were found to be minimal on COD reduction and are therefore covered in Supplementary data.*

As can be seen from Figure 2, COD removal increased from 1 to 60% and from 5 to 18% for the non-preheated and preheated oxidant scenarios, as the temperature was increased from 300°C to 380°C. At temperatures above 340°C, the presence of reactive free hydroxyl radicals formed in non-preheated oxidant configuration enhances the conversion efficiency. However, below 340°C, the temperature of the downward flow is well below the critical temperature of water (i.e. a down flow temperature of 345-370°C equates to a post mixed temperature of 300-340°C). Therefore, there is not enough energy to break down the organic or the oxidant mixture which result in a low COD removal for the non-preheated oxidant configuration. However, as the temperature of the heated down flow reaches the critical point, there are significant increases in COD removal. A high COD reduction of >50% at such low

temperatures and residence times, particularly when compared to other studies [49, 50], might result from the immediate and rapid heating of the organic and oxidant solution within the counter-current mixing reactor in addition to the instantaneous strong and uniform mixing of upward and downward streams [39].

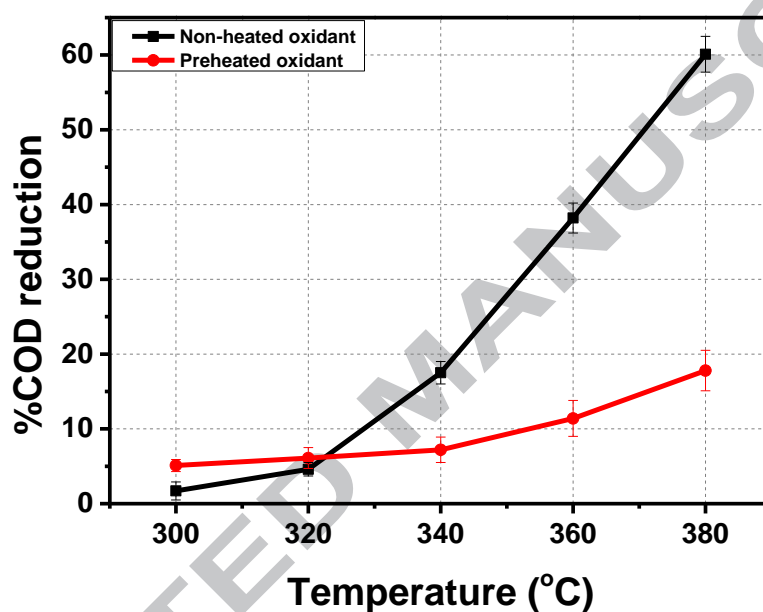


Figure 2: The effect reaction temperature on %COD removal. All experiments were carried out at 25.0 MPa, a residence time of 1.5 sec, an initial acrylic acid concentration of 10 mM and an oxidant ratio of 1

3.2 The effect of oxidant excess on COD reduction

Minimal COD reduction was achieved at 380°C without the addition of an oxidant (Figure 3).

It is therefore reasonable to assume that the effect of the hydrolysis reaction on acrylic acid was negligible, and that the oxidation reaction alone is responsible for its removal. Oxidant ratio was altered from 0-3 at fixed operating conditions of 380°C and 25.0 MPa with an initial concentration of 10 mM and 0.75 sec residence time. Figure 3 shows that COD

removal rapidly increases with excess oxidant particularly in the case of the non-heated oxidant configuration. The reduction rate appears to plateau above an oxidant ratio of 2.0 which is in agreement with the findings of Shin et al. [51] and although their residence times were significantly longer than 0.75 seconds.

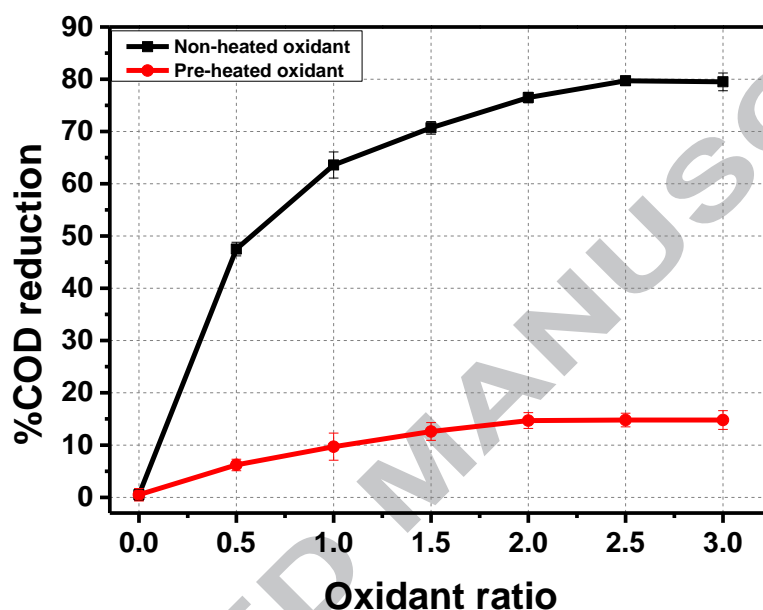


Figure 3: The effect of oxidant ratio on COD removal efficiency at 380°C, 25.0 MPa and 10mM acrylic acid.

3.3 The impact of in-situ nano-catalyst formation

A series of experiments was carried out to investigate whether the addition of various metal salt solutions would impact on COD reduction. In principle these metal salts form nanoparticles, via the SCWHS process [52]. These newly formed metal oxides nanoparticles would then act as catalysts during the decomposition of acrylic acid. Figure 4 shows the catalytic effect of each metal oxide on COD removal compared to the catalyst free reactions at both sub- (4a and 4c) and supercritical (4b and 4d) temperatures. Chromium oxide appears to show the most significant improvement in COD reduction at supercritical temperatures,

with both the preheated and non-preheated scenarios. TiO_2 shows the lowest activity of the tested materials.

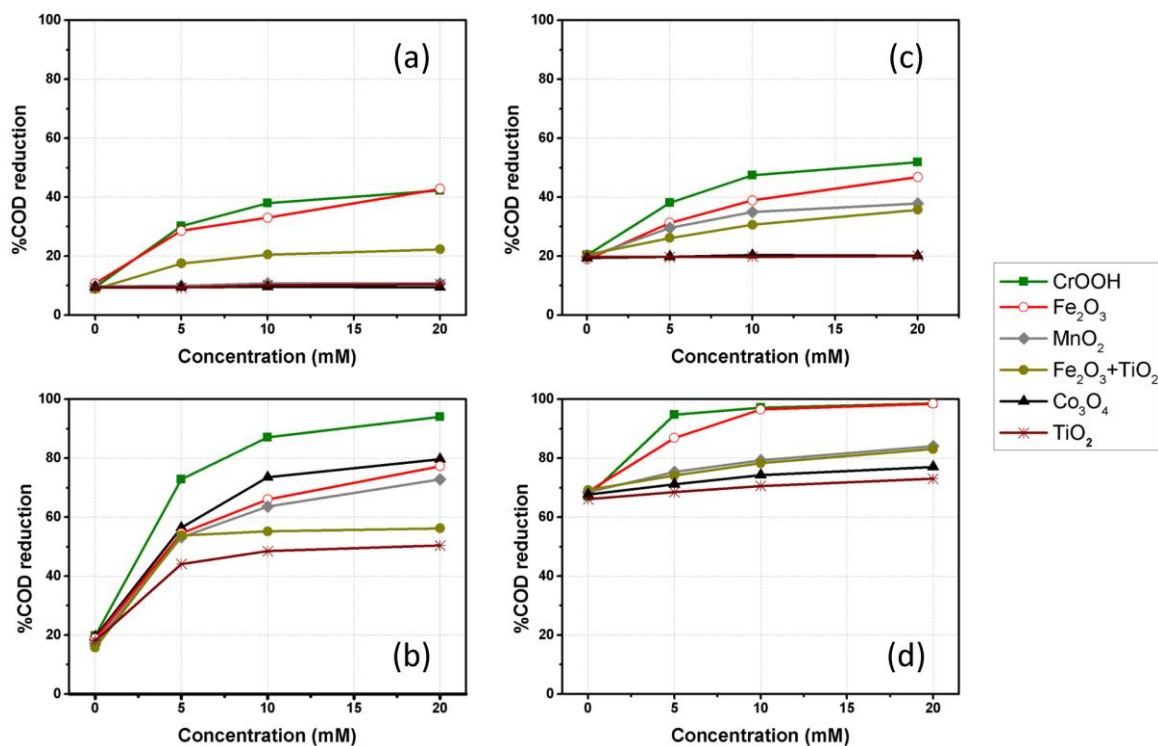


Figure 4: Catalytic effect of metal oxide nanoparticles on %COD removal at 25.0 MPa, oxidant ratio of 1 and initial acrylic acid concentration of 10mM. (a) at 340°C, preheated configuration, (b) at 380°C preheated configuration, (c) at 340°C non-preheated configuration and (d) at 380°C non-preheated configuration.

Hematite significantly improves the removal rate of acrylic acid at both temperatures but specifically with more than 95% COD reduction in the non-preheated oxidant configuration.

It is worth mentioning that, part of the high COD removal is also due to the Fenton reaction between H_2O_2 and the iron(III) present in the solution [53]. Cobalt oxide shows a high catalytic activity with a 61% increase over the non-catalysed reaction especially in the preheated oxidant arrangement where its activity is obviously higher compared with the non-preheated oxidant scenario. Interestingly, it has no effect at subcritical temperatures. MnO_2 is

generally considered to be one of the most active and stable catalysts during phenol oxidation [54]. In Figure 4d the MnO_2 catalyst showed a 77.3 and 84.1% of COD reduction in the preheated and non-preheated oxidant configurations, respectively. There are other interesting possibilities with the combination of catalysts e.g. whilst TiO_2 appeared to have relatively low catalytic affect, its combination with Fe_2O_3 enhanced the final settling rate in the effluent. Hematite, when on its own, was relatively stable in the effluent which would present practical issues with scale up of the process.

The catalytic preheated oxidant configuration showed highest activity when operating at supercritical temperatures. As discussed previously, O_2 is a weak oxidant at moderate temperatures (e.g. $<400^\circ\text{C}$) (28), so the addition of catalyst clearly improves the overall reduction rate. For the catalytic preheated oxidation, the oxidation is most probably initiated by the adsorption of reactant species on the catalyst surface. Oxygen adsorbed at the catalyst surface is present mainly as the superoxide ion O_2^- which may decompose further with the formation of the O^- ion [55]. The radical ion forms O^- and O_2^- which possess even higher oxidative activities than OH^\bullet radicals [56]. As such, this combined approach with catalysts in-situ presents a new approach to enhanced COD reduction although more work is necessary to understand the kinetic mechanisms at work. Homogeneous and heterogeneous catalysis reactions may well create the synergetic effects where the metal salts and subsequent metal oxide products both act as catalysts during the destruction of acrylic acid at supercritical conditions.

3.4 Characterization of the nanocatalyst product

Figure 5 shows the representative XRD profiles for each catalyst in Section 3.3. The XRD patterns show that the obtained particles are TiO_2 , Fe_2O_3 , and Co_3O_4 . For experiments with Cr salt addition, all products showed a transparent green colour and, when tested with a laser pointer (Figure S3 in supplementary data), showed a positive beam path which normally indicates the presence of nanoparticles. However, the XRD patterns show no crystalline or amorphous phase of chromium oxide. TEM images of each nanomaterial produced (in both configurations) are shown in Figures 6a-b. The morphology in most cases appears to be spherical with detectable edges and (in most cases) crystallinity. Table 1 gives the crystal sizing data from XRD and TEM analysis using Scherrer equation and ImageJ software and over 100 measurements. Cr based particles were very small via TEM - and that is one the most important factors that increase the catalytic activity of metal nanoparticles. Cr_2O_3 has been synthesised hydrothermally at milder conditions i.e. 180°C in batch, but only in the presence of urea[57], so it is more likely that these particles observed using TEM were either CrOOH or $\text{Cr}(\text{OH})_3$ particles. There are other papers to support the assumption that this greenish suspension is the Cr equivalent of boehmite (AlOOH). Most researchers conclude that a minimum of 450°C is required to convert the CrOOH to Cr_2O_3 [58, 59] which is higher than the experiments in this paper. However, the CrOOH is clearly the best catalyst in this work.

Table 1: Crystal size (nm) of in-situ metal oxides formed during SCWO.

Catalyst Type	Preheated oxidant scenario		Non-preheated oxidant scenario	
	<i>Scherrer</i> (nm)	<i>ImageJ</i> (nm)	<i>Scherrer</i> (nm)	<i>ImageJ</i> (nm)
TiO ₂	7.7	8.0	7.5	9.0
Fe ₂ O ₃	25.5	26.5	21.8	16.1
Co ₃ O ₄	23.3	35.4	20.4	15.8
CrOOH	-	5.0	-	6.0
MnO ₂	-	19.0	-	20.6
Fe ₂ O ₃ + TiO ₂	-	13.0	-	14.6

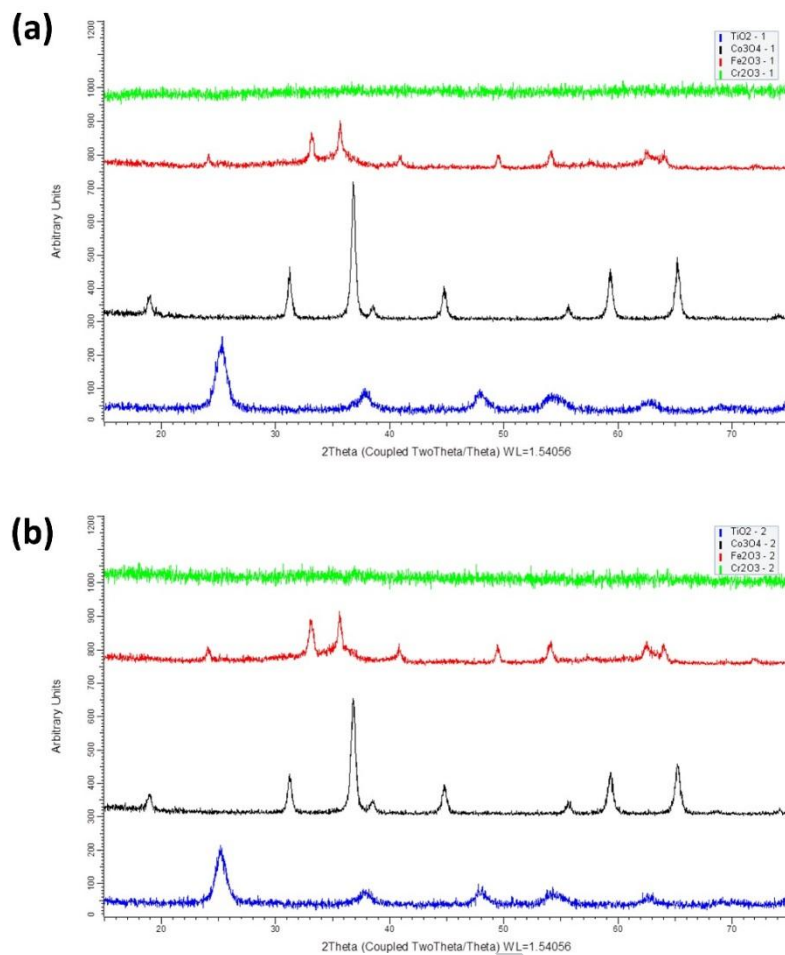


Figure 5: XRD profiles of the metal oxide nanoparticles obtained at 380°C, 25.0 MPa, oxidant ratio of 1.5 and 0.02M of metal salt concentration. (a) Preheated oxidant and (b) Non-preheated oxidant scenario.

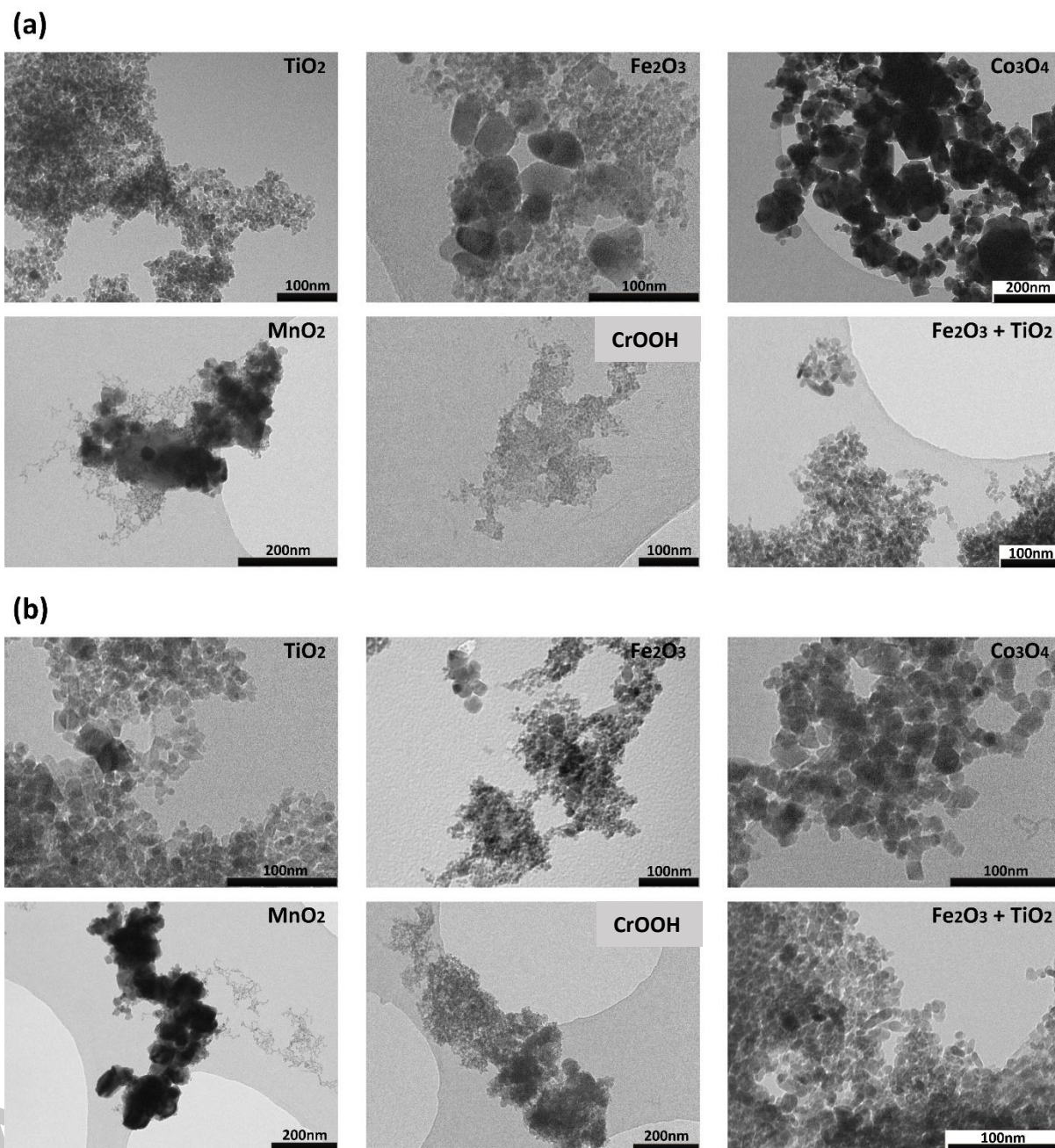


Figure 6: TEM images of the metal oxide nanoparticles obtained at 380°C, 25.0 MPa, oxidant ratio of 1.5 and 0.02M of metal salt concentration. (a) Preheated oxidant and (b) Non-preheated oxidant scenario.

3.5 Initial economic considerations for the benefits of a combined SCWO/CHS approach

An initial simulation and economic study was carried out on the combined SCWO/SCWHS process to better understand the advantages that might be presented at industrial scale. These studies were based on an actual industrial scale plant, which was designed and constructed during the SHYMAN project [60]. An Aspen Plus[®] simulation used the flow rates of 3:1.5 m³/h (downflow of supercritical water: upflow of acrylic acid in water) and the reaction pressure at 25.0 MPa.

Three different scenarios are modelled using Aspen Plus[®] software to achieve a COD removal of 98%: pre-heated, non-preheated and catalytic non-preheated oxidant configuration (using Fe(NO₃)₃·9H₂O). Whilst CrOOH was the better catalyst, the iron nitrate precursor is significantly cheaper and Fe₂O₃ is more environmentally benign[61].

For calculating the necessary temperature to get 98% of conversion, the experimental results shown in Figure 2 were extrapolated with polynomial equations and the temperatures for the pre-heated and non-preheated oxidant process found to be 498°C and 401°C, respectively. These conditions were chosen because the catalytic non-preheated oxidant configuration, already showed that a 98% reduction of COD was possible at 380°C (see Figure 4).

Figure 7 shows the main simulated process using Aspen Plus[®] software. Mass balances are given in Supplementary data S1.4. In pre-heated configuration, the organic solution is fed in via stream 9₁ and enters at the bottom end of the reactor via stream 11₁. The oxidant solution is introduced in the reactor by stream 13₁ at the top end. This stream is heated in a heat exchanger followed by a gas-fired boiler using natural gas (NG). Regarding non-preheated oxidant configuration the flow diagram is the same but in this case, the oxidant is fed by stream 9₁ and stream 13₁ consists of process water. Finally, using catalytic configuration, the metal salt is supplied from stream 9₂.

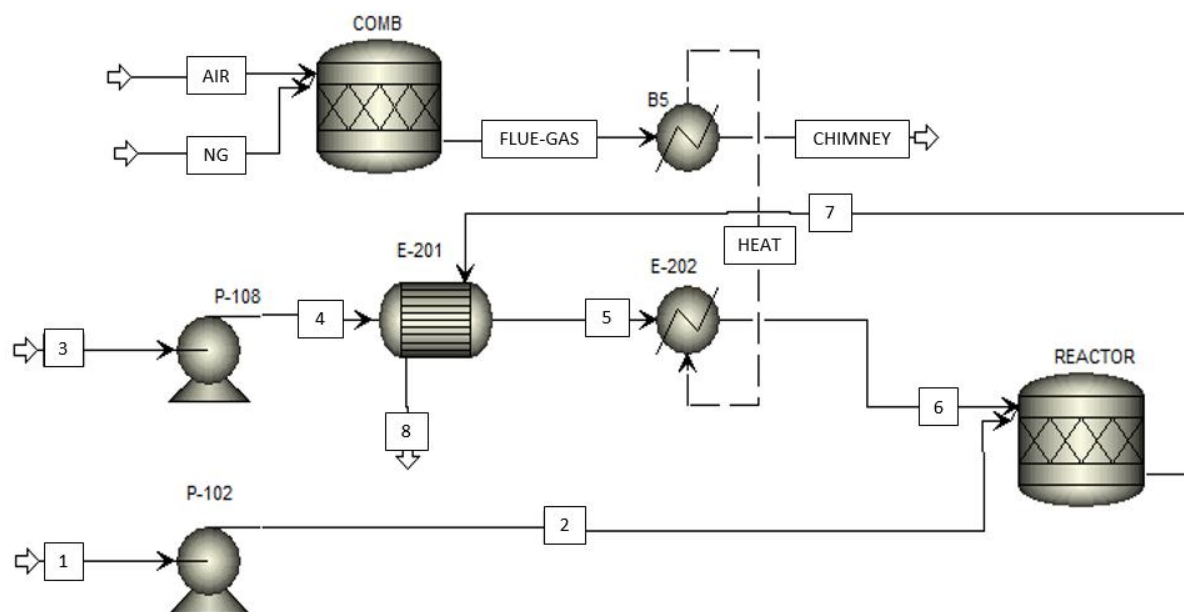


Figure 7. Flow diagram of the industrial scale process (Aspen Plus® software)

With the objective of studying the economic feasibility of each configuration in the industrial plant, the energy requirements are compared in Figure 8. The capital expenditure (CAPEX) is the effectively the same in three configurations with the same number of pumps, heaters etc. and the assumption is that none of the configurations will cause specific long term issues with operation. From Figure 8 the electricity requirement by the pumps are essentially equivalent in all three configurations. However, the natural gas requirement is dependent on the temperature required to achieve 98% conversion. Therefore, in pre-heated oxidant configuration the natural gas requirement is the highest, at about 1160 kW.

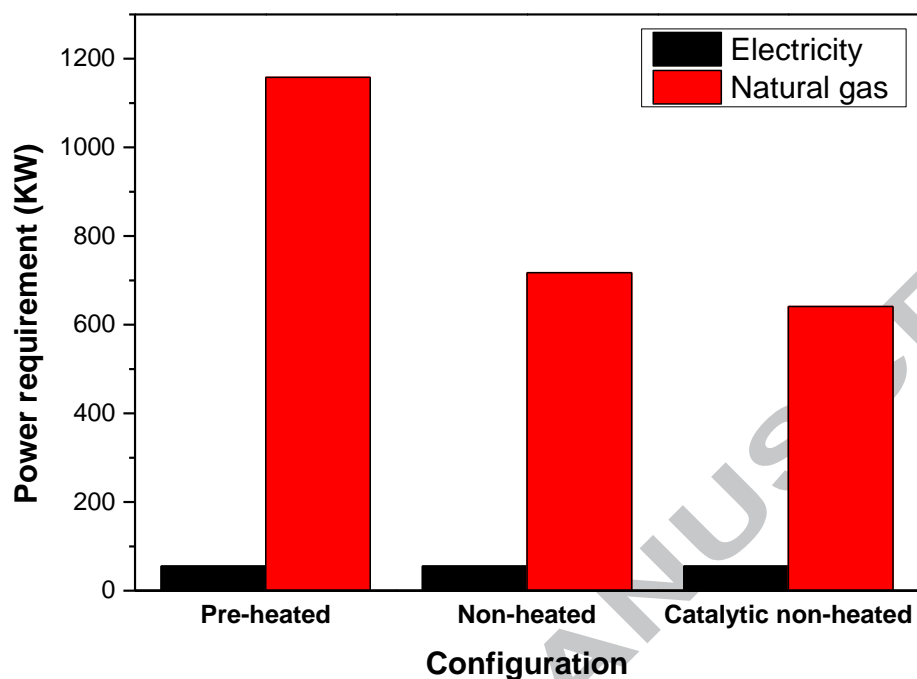


Figure 8: Energy calculations for demand for energy demand for the three scenarios

Water costs 1.92 £/m³, and hydrogen peroxide is 0.32 £/kg. In the United Kingdom electricity is costed at 0.12 £/kW and natural gas is 0.055 £/kW. Thus, the costs calculated for pre-heated and non-preheated oxidant configuration on an industrial scale plant are about 85 £/h and 61 £/h, respectively, as shown in Table 2.

Table 2: Cost of preheated and non-preheated oxidant configurations.

Preheated					
	H ₂ O (l/h)	H ₂ O ₂ (kg/h)	Natural Gas (kW)	Electricity (kW)	Total cost (£/h)
Flow	3807	22.95	1158.0	55.6	85.01
Cost (£/h)	7.31	7.34	63.7	6.7	
Total cost (£/kg contaminant-water)			£0.067		
Non-preheated					
	H ₂ O (l/h)	H ₂ O ₂ (kg/h)	Natural Gas (kW)	Electricity (kW)	Total cost (£/h)
Flow	3807	22.95	717.4	55.6	60.78
Cost (£/h)	7.31	7.34	39.5	6.7	
Total cost (£/kg contaminant-water)			£0.048		

With the catalytic configuration (Table 3), it must be noted the iron nitrate precursor price is 0.84 £/kg (from molbase.com) bringing the total cost to 67 £/h. This is more than the non-preheated case. However, in this case, Fe₂O₃ nanoparticles are also produced. Economic calculations should therefore take into account the value of this nanomaterial which, at almost 2.0 kg/hr and a relatively conservative value of £30/kg would certainly negate any basic operating expenditure (OPEX).

Table 3: Cost of catalytic non-preheated oxidant configuration.

Non-preheated + catalyst						
	H ₂ O (L/h)	H ₂ O ₂ (kg/h)	Fe(NO ₃) ₃ .H ₂ O (kg/h)	Natural Gas (kW)	Electricity (kW)	Total cost (£/h)
Flow	3803.39	22.95	12.12	640.93	55.59	66.80
Cost (£/h)	7.30	7.34	10.23	35.25	6.67	
Total cost (£/kg contaminant-water)				0.053		

4. Conclusions

The counter current reactor was designed to produce short residence times and rapid mixing of two different fluids and (whilst most SCWO reactors use substantial residence times and high times) COD reduction was shown to be relatively high (up to 80%).

The oxidant (H_2O_2) delivery method was found to have a large impact on removal efficiency and reaction temperature was also a key variable. At 380 °C and 25.0 MPa, the non-preheated oxidant configuration with a residence time of 0.75 sec resulted in an 80% COD removal as opposed to a 15% COD removal with the equivalent preheated oxidant experiment. The difference between the efficiency for the two methods is linked to the availability of $\cdot\text{OH}$ radicals and/or molecular oxygen, respectively.

The addition of small amounts of metal salts in the upflow also led to a reduction in COD levels. These precursors created metal oxide or oxyhydroxide nanoparticles in situ which enhanced the oxidation efficiency. Fe_2O_3 and CrOOH were the most significant catalysts, increasing COD reduction to more than 98% at a temperature of 380°C and a residence time of less than 1 sec.

From a basic OPEX analysis, the best option is the non-preheated catalytic configuration because the temperatures required to achieve high levels of COD reduction were much lower than the other configurations. The basic economic impact of catalyst addition was also assessed to be favourable. The secondary value of any nano-catalyst bi-product could potentially outweigh any OPEX costs for the SCWO process itself. There is also a clear opportunity to increase the metal precursor concentration, which would not impact on removal rates of the contaminant but would increase the quantity of the nano bi-product, further increasing the financial viability of the combined process.

Acknowledgments

We thank the European Union's Seventh Framework Programme (FP7/2007–2013), grant agreement no. FP7-NMP4-LA-2012-280983, the SHYMAN project and the Iraqi Council of Representatives for the PhD scholarship for Mr Al-Atta. Y.G.R. thanks FPI-UVa program for scholarship and UVa mobility program 2016-17. Nigel Neate and Rhys W. Lodge in the Nanoscale and Microscale Research Centre are gratefully acknowledged for the use of XRD and TEM facilities.

References

- [1] Z. Fang, *Near-critical and Supercritical Water and Their Applications for Biorefineries*, Springer, 2014.
- [2] P.A. Marrone, Supercritical water oxidation—current status of full-scale commercial activity for waste destruction, *The Journal of Supercritical Fluids* 79 (2013) 283-288.
- [3] S. Zhang, Z. Zhang, R. Zhao, J. Gu, J. Liu, B. Örmeci, J. Zhang, A Review of Challenges and Recent Progress in Supercritical Water Oxidation of Wastewater, *Chemical Engineering Communications* 204 (2017) 265-282.
- [4] H. Weingärtner, E.U. Franck, *Supercritical Water as a Solvent*, *Angewandte Chemie International Edition* 44 (2005) 2672-2692.
- [5] A. Kruse, E. Dinjus, Hot compressed water as reaction medium and reactant: properties and synthesis reactions, *The Journal of Supercritical Fluids* 39 (2007) 362-380.
- [6] L. Qian, S. Wang, D. Xu, Y. Guo, X. Tang, L. Wang, Treatment of municipal sewage sludge in supercritical water: a review, *Water research* 89 (2016) 118-131.
- [7] R. Piñero-Hernanz, C. Dodds, J. Hyde, J. García-Serna, M. Poliakoff, E. Lester, M.J. Cocero, S. Kingman, S. Pickering, K.H. Wong, Chemical recycling of carbon fibre reinforced composites in nearcritical and supercritical water, *Composites Part A: Applied Science and Manufacturing* 39 (2008) 454-461.
- [8] J. Queiroz, M. Bermejo, F. Mato, M. Cocero, Supercritical water oxidation with hydrothermal flame as internal heat source: Efficient and clean energy production from waste, *The Journal of Supercritical Fluids* 96 (2015) 103-113.
- [9] P.W. Dunne, C.L. Starkey, A.S. Munn, S.V. Tang, O. Luebben, I. Shvets, A.G. Ryder, Y. Casamayou-Boucau, L. Morrison, E.H. Lester, Bench-and Pilot-Scale Continuous-Flow Hydrothermal Production of Barium Strontium Titanate Nanopowders, *Chemical Engineering Journal* (2015).
- [10] M. Bermejo, M. Cocero, Supercritical water oxidation: a technical review, *AIChE Journal* 52 (2006) 3933-3951.
- [11] V. Marulanda, G. Bolaños, Supercritical water oxidation of a heavily PCB-contaminated mineral transformer oil: Laboratory-scale data and economic assessment, *The journal of supercritical fluids* 54 (2010) 258-265.
- [12] S. Falamarzian, O. Tavakoli, R. Zarghami, M.A. Faramarzi, Catalytic hydrothermal treatment of pharmaceutical wastewater using sub-and supercritical water reactions, *The Journal of Supercritical Fluids* 95 (2014) 265-272.
- [13] D. Xu, S. Wang, J. Zhang, X. Tang, Y. Guo, C. Huang, Supercritical water oxidation of a pesticide wastewater, *Chemical Engineering Research and Design* 94 (2015) 396-406.
- [14] B. Veriansyah, J.-D. Kim, J.-C. Lee, Supercritical water oxidation of thiodiglycol, *Industrial & engineering chemistry research* 44 (2005) 9014-9019.
- [15] A. Leybros, A. Roubaud, P. Guichardon, O. Boutin, Ion exchange resins destruction in a stirred supercritical water oxidation reactor, *The Journal of Supercritical Fluids* 51 (2010) 369-375.
- [16] B. Al-Duri, F. Alsoqyani, I. Kings, Supercritical water oxidation for the destruction of hazardous waste: better than incineration, *Phil. Trans. R. Soc. A* 373 (2015) 20150013.
- [17] V. Vadillo, J. Sánchez-Oneto, J.R.n. Portela, E.J. Martínez de la Ossa, Problems in supercritical water oxidation process and proposed solutions, *Industrial & Engineering Chemistry Research* 52 (2013) 7617-7629.
- [18] M. Sun, X. Wu, Z. Zhang, E.-H. Han, Oxidation of 316 stainless steel in supercritical water, *Corrosion science* 51 (2009) 1069-1072.
- [19] X. Tang, S. Wang, D. Xu, Y. Gong, J. Zhang, Y. Wang, Corrosion behavior of Ni-based alloys in supercritical water containing high concentrations of salt and oxygen, *Industrial & Engineering Chemistry Research* 52 (2013) 18241-18250.

- [20] F.J. Rivas, S.T. Kolaczowski, F.J. Beltran, D.B. McLurgh, Hydrogen peroxide promoted wet air oxidation of phenol: influence of operating conditions and homogeneous metal catalysts, *J. Chem. Technol. Biotechnol.* 74 (1999) 390-398.
- [21] S. Kolaczowski, F. Beltran, D. McLurgh, F. Rivas, Wet air oxidation of phenol: factors that may influence global kinetics, *Process safety and environmental protection* 75 (1997) 257-265.
- [22] A. Quintanilla, J. Casas, J. Rodriguez, Hydrogen peroxide-promoted-CWAO of phenol with activated carbon, *Applied Catalysis B: Environmental* 93 (2010) 339-345.
- [23] S. Wang, Y. Guo, L. Wang, Y. Wang, D. Xu, H. Ma, Supercritical water oxidation of coal: Investigation of operating parameters' effects, reaction kinetics and mechanism, *Fuel Processing Technology* 92 (2011) 291-297.
- [24] F. Vogel, J. Harf, A. Hug, P.R. Von Rohr, Promoted oxidation of phenol in aqueous solution using molecular oxygen at mild conditions, *Environmental progress* 18 (1999) 7-13.
- [25] T.M. Hayward, I.M. Svishchev, R.C. Makhija, Stainless steel flow reactor for supercritical water oxidation: corrosion tests, *The Journal of supercritical fluids* 27 (2003) 275-281.
- [26] P.W. Dunne, A.S. Munn, C.L. Starkey, T.A. Huddle, E.H. Lester, Continuous-flow hydrothermal synthesis for the production of inorganic nanomaterials, *Phil. Trans. R. Soc. A* 373 (2015) 20150015.
- [27] H. Hayashi, Y. Hakuta, Hydrothermal Synthesis of Metal Oxide Nanoparticles in Supercritical Water, *Materials* 3 (2010) 3794-3817.
- [28] G. Aksomaityte, M. Poliakoff, E. Lester, The production and formulation of silver nanoparticles using continuous hydrothermal synthesis, *Chemical engineering science* 85 (2013) 2-10.
- [29] P.W. Dunne, C.L. Starkey, M. Gimeno-Fabra, E.H. Lester, The rapid size-and shape-controlled continuous hydrothermal synthesis of metal sulphide nanomaterials, *Nanoscale* 6 (2014) 2406-2418.
- [30] E. Lester, S.V. Tang, A. Khlobystov, V.L. Rose, L. Buttery, C.J. Roberts, Producing nanotubes of biocompatible hydroxyapatite by continuous hydrothermal synthesis, *CrystEngComm* 15 (2013) 3256-3260.
- [31] I. Clark, P.W. Dunne, R.L. Gomes, E. Lester, Continuous Hydrothermal Synthesis of Ca₂Al-NO₃ Layered Double Hydroxides: The Impact of Reactor Temperature, Pressure and NaOH Concentration on Crystal Characteristics, *J. Colloid Interface Sci.* (2017).
- [32] A. Munn, P.W. Dunne, S. Tang, E. Lester, Large-scale continuous hydrothermal production and activation of ZIF-8, *Chemical communications* 51 (2015) 12811-12814.
- [33] A. Miller, R. Espanani, A. Junker, D. Hendry, N. Wilkinson, D. Bollinger, J. Abelleira-Pereira, M. Deshusses, E. Inniss, W. Jacoby, Supercritical water oxidation of a model fecal sludge without the use of a co-fuel, *Chemosphere* 141 (2015) 189-196.
- [34] A. Gidner, L. Stenmark, Supercritical water oxidation of sewage sludge—State of the art, *Proceedings of the IBC's Conference on Sewage Sludge and Disposal Options*, 2001.
- [35] S.A. Pisharody, J.W. Fisher, M.A. Abraham, Supercritical water oxidation of solid particulates, *Industrial & engineering chemistry research* 35 (1996) 4471-4478.
- [36] M.D. LaGrega, P.L. Buckingham, J.C. Evans, *Hazardous waste management*, Waveland Press 2010.
- [37] P. Kumar, P. Raghavendra, S. Chand, Catalytic wet air oxidation of carboxylic acid present in wastewater, *JOURNAL OF SCIENTIFIC AND INDUSTRIAL RESEARCH* 65 (2006) 838.
- [38] R.V. Shende, J. Levec, Subcritical aqueous-phase oxidation kinetics of acrylic, maleic, fumaric, and muconic acids, *Industrial & engineering chemistry research* 39 (2000) 40-47.
- [39] E. Lester, P. Blood, J. Denyer, D. Giddings, B. Azzopardi, M. Poliakoff, Reaction engineering: The supercritical water hydrothermal synthesis of nano-particles, *The Journal of Supercritical Fluids* 37 (2006) 209-214.
- [40] P.E. Savage, A perspective on catalysis in sub-and supercritical water, *The Journal of Supercritical Fluids* 47 (2009) 407-414.

- [41] J. Sierra-Pallares, T. Huddle, E. Alonso, F.A. Mato, J. García-Serna, M.J. Cocero, E. Lester, Prediction of residence time distributions in supercritical hydrothermal reactors working at low Reynolds numbers, *Chemical Engineering Journal* 299 (2016) 373-385.
- [42] T. Huddle, A. Al-Atta, S. Moran, E. Lester, Pseudo fluid modelling used in the design of continuous flow supercritical water oxidation reactors with improved corrosion resistance, *The Journal of Supercritical Fluids* 120 (2017) 355-365.
- [43] T. Wu, J.D. Englehardt, A new method for removal of hydrogen peroxide interference in the analysis of chemical oxygen demand, *Environmental science & technology* 46 (2012) 2291-2298.
- [44] E. Lee, H. Lee, Y. Kim, K. Sohn, K. Lee, Hydrogen peroxide interference in chemical oxygen demand during ozone based advanced oxidation of anaerobically digested livestock wastewater, *International Journal of Environmental Science & Technology* 8 (2011) 381-388.
- [45] J. Sierra-Pallares, T. Huddle, J. García-Serna, E. Alonso, F. Mato, I. Shvets, O. Luebben, M.J. Cocero, E. Lester, Understanding bottom-up continuous hydrothermal synthesis of nanoparticles using empirical measurement and computational simulation, *Nano Research* 9 (2016) 3377-3387.
- [46] Y.H. Shin, N.C. Shin, B. Veriansyah, J. Kim, Y.-W. Lee, Supercritical water oxidation of wastewater from acrylonitrile manufacturing plant, *J. Hazard. Mater.* 163 (2009) 1142-1147.
- [47] B. Veriansyah, J.-D. Kim, J.-C. Lee, Destruction of chemical agent simulants in a supercritical water oxidation bench-scale reactor, *J. Hazard. Mater.* 147 (2007) 8-14.
- [48] L.D. Pinto, L.M.F. dos Santos, B. Al-Duri, R.C. Santos, Supercritical water oxidation of quinoline in a continuous plug flow reactor—part 1: effect of key operating parameters, *J. Chem. Technol. Biotechnol.* 81 (2006) 912-918.
- [49] W.-J. Gong, F. Li, D.-L. Xi, Supercritical water oxidation of acrylic acid production wastewater in transpiring wall reactor, *Environmental Engineering Science* 26 (2009) 131-136.
- [50] L. Wang, S. Wang, Y. Li, T. Zhang, J. Yang, M. Wang, Supercritical Water Oxidation of acrylic acid wastewater and sludge, *Resources, Environment and Engineering II: Proceedings of the 2nd Technical Congress on Resources, Environment and Engineering (CREE 2015, Hong Kong, 25-26 September 2015)*, CRC Press, 2015, pp. 459.
- [51] Y.H. Shin, N.C. Shin, B. Veriansyah, J. Kim, Y.-W. Lee, Supercritical water oxidation of wastewater from acrylonitrile manufacturing plant, *J. Hazard. Mater.* 163 (2009) 1142-1147.
- [52] Y.Z. Zhu, S. Takami, G.Y. Seong, M. Dejhosseini, M.Z. Hossain, T. Noguchi, D. Hojo, N. Aoki, T. Aida, T. Adschiri, Green solvent for green materials: a supercritical hydrothermal method and shape-controlled synthesis of Cr-doped CeO₂ nanoparticles, *Philos. Trans. R. Soc. A-Math. Phys. Eng. Sci.* 373 (2015) 14.
- [53] H.B. Dunford, Oxidations of iron (II)/(III) by hydrogen peroxide: from aquo to enzyme, *Coordination Chemistry Reviews* 233 (2002) 311-318.
- [54] K. Tomita, Y. Oshima, Stability of manganese oxide in catalytic supercritical water oxidation of phenol, *Industrial & engineering chemistry research* 43 (2004) 7740-7743.
- [55] M. Krajnc, J. Levec, Oxidation of phenol over a transition-metal oxide catalyst in supercritical water, *Industrial & engineering chemistry research* 36 (1997) 3439-3445.
- [56] Y. Wang, S. Wang, Y. Guo, D. Xu, Y. Gong, X. Tang, H. Ma, Oxidative degradation of lurgi coal-gasification wastewater with Mn₂O₃, Co₂O₃, and CuO catalysts in supercritical water, *Industrial & Engineering Chemistry Research* 51 (2012) 16573-16579.
- [57] S. Rajagopal, M. Bharaneswari, D. Nataraj, O.Y. Khyzhun, Y. Djaoued, Crystal structure and electronic properties of facile synthesized Cr₂O₃ nanoparticles, *Materials Research Express* 3 (2016).
- [58] P. Pardo, J.M. Calatayud, J. Alarcón, Chromium oxide nanoparticles with controlled size prepared from hydrothermal chromium oxyhydroxide precursors, *Ceramics International* 43 (2017) 2756-2764.
- [59] P. Gibot, L. Vidal, Original synthesis of chromium (III) oxide nanoparticles, *Journal of the European Ceramic Society* 30 (2010) 911-915.

[60] B. Stieberova, M. Zilka, M. Ticha, F. Freiberg, P. Caramazana-González, J. McKechnie, E. Lester, Application of ZnO Nanoparticles in a Self-cleaning Coating on a Metal Panel: An Assessment of Environmental Benefits, *ACS Sustainable Chemistry and Engineering* 5 (2017) 2493-2500.

[61] K. Murugesan, T. Senthamarai, M. Sohail, M. Sharif, N.V. Kalevaru, R.V. Jagadeesh, Stable and reusable nanoscale Fe₂O₃-catalyzed aerobic oxidation process for the selective synthesis of nitriles and primary amides, *Green Chem.* 20 (2018) 266-273.

HIGHLIGHTS

- A combined oxidation/synthesis process for contaminant removal
- Lower temperature requirements for contaminant removal compared to other papers
- A comparison of the effectiveness of different nanocatalysts in contaminant removal
- Experiments to show how oxidant addition impacts on contaminant removal efficiency
- An initial techno-economic assessment showing benefits of the process vs current standards

GRAPHICAL ABSTRACT

